# Designer Self-Assembling Peptide Nanofiber Scaffolds

**Shuguang Zhang, Hidenori Yokoi, Fabrizio Gelain, and Akihiro Horii**

## 1 Introduction

Nearly all tissue cells are embedded in 3-D microenvironment in the body surrounded by nanoscale extracellular matrix. On the other hand, nearly all tissue cells have been studied in 2-D using Petri dishes, multi-well plates or glass slides coated with various substrates. How can one reconcile the apparent disparity? Likewise, although millions of cell biology papers have been published using the 2-D culture systems, one must ask how we can be so certain the results obtained from the 2-D system truly reflect the in vivo conditions. Science, after all, is to constantly ask questions, big and small. As the late legendary Francis Crick eloquently put it "You should always ask questions, the bigger the better. If you ask big questions, you get big answers."

## 2 Two D or Not Two D

Although Petri dish has had an enormous impact on modern biology, the flat bottom nature of the Petri dish culture system, including multi-well plates, glass coverslips, etc., is less than ideal for study tissue cells for several reasons: (1) It is a 2-D system, which is in sharp contrast to the 3-D environment of natural tissues both in animals and plants. (2) The Petri dish flat surface without coating is rigid and inert, again in sharp contrast to the in vivo environment where cells intimately interact with the

S. Zhang (✉) • H. Yokoi • F. Gelain • A. Horii
Center for Biomedical Engineering, Center for Bits & Atoms
Massachusetts Institute of Technology, Cambridge, MA, USA
e-mail: shuguang@mit.edu

G.A. Silva and V. Parpura (eds.), *Nanotechnology for Biology and Medicine: At the Building Block Level*, Fundamental Biomedical Technologies,
DOI 10.1007/978-0-387-31296-5_6, 

extracellular matrix and with each other. (3) The tissue cell monolayers on coated 2-D surface, such as poly-L-lysine, collagen gels, fibronectin, laminin, and Matrigel (Kleinman et al. 1986; Kleinman and Martin 2005) as well as other synthetic materials containing segments of adhesion motifs, have only part of the cell surface attached to the materials and interact with neighboring cells. The remaining parts are often directly exposed to the culture media, unlike the majority of tissue environment where every cell intimately interacts with its neighbor cells and extracellular matrix; of course, there are exceptions to such general statement, e.g., airway epithelial cells. Thus 3-D-matrix interactions display enhanced cell biological activities. (4) The transport phenomena of 2-D and 3-D are drastically different. In 2-D culture systems, cytokines, chemokines and growth factors quickly diffuse in the media across the culture dish. This is again in sharp contrast to the in vivo environment where chemical and biological gradient diffusion systems play a vital role in signal transduction, cell–cell communications and development. (5) Cells cultured on a 2-D Petri dish are not readily transportable, that is, it is nearly impossible to move cells from one environment to another without incurring changes in the cell–material and cell–cell interactions. For example, cell collections using trypsinization or mechanically using cell scrapers may have adverse effect on cell–materials/environment interactions. In contrast, cells cultured on 3-D scaffolds are more readily transportable without significantly harming cell–material and cell–cell interactions, thus providing a significantly new way to study cell biology.

## 3 Micro- and Nanoscales: Why Are They Important?

The importance of length scales is apparent, for example, when considering the scales of trees and grasses (Fig. 1). Both are made of the same basic building blocks; sugars that are polymerized by enzymes to produce cellulose fibers. Trees, usually 20–40 cm in diameter, are common in forests. If animals are in the forest, they can either go between the trees or climb onto the trees, they cannot go cross through the trees because animals are similar in scales as the trees. On the other hand, grasses are usually 0.5 cm (commonly 0.3–1 cm in diameter) in diameter. Animals can be fully embedded in and surrounded by high grass, yet can move freely within the high grass field. Perhaps, this analogy can be extended to scaffolds of various scales for cells. Cells are commonly micrometer-scales, 5–20 μm, objects. When cells are residing on microfiber polymers, they are about same scales as the microfibers. When the cells are in the extracellular matrix, they are embedded within the nanofiber matrix, which they exceed in size by a factor of ~1,000.

In the last three decades, several biopolymers, including poly-L-lactide acid (PLLA), poly-lactic-co-glycolic acid (PLGA), PLLA–PLGA copolymers and other biomaterials including alginate, agarose, collagen gels and others, have been developed to culture cells in 3-D (Ratner et al. 1996; Lanza et al. 2000; Yannas 2001; Atala and Lanza 2002; Hoffman 2002; Palsson et al. 2003). These culture systems have significantly advanced our understanding of cell–material interactions and

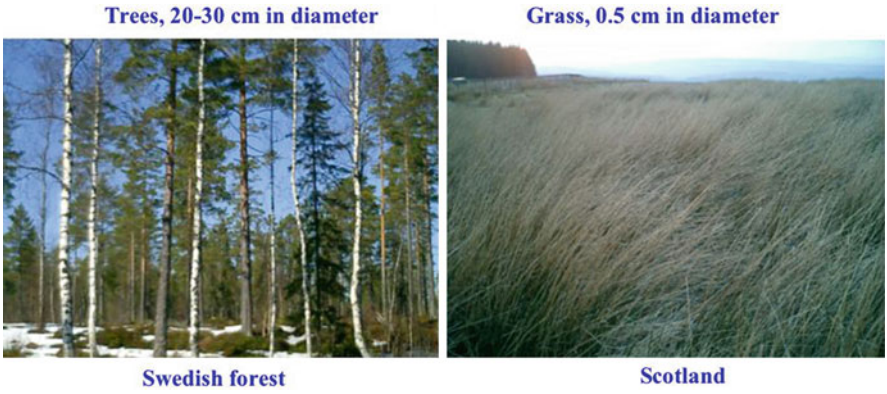


**Fig. 1** The drastic difference in scales. Both trees and grass are made of cellulose, but they have different sizes. The trees shown on the *left* are 20–30 cm in diameter and the distances between the trees are in tens of meters. Animals cannot walk through the trees but between them. Some animals can climb on the trees (*left panel*). In analogy to cells which are ~5–20 μm in size, and can only attach to the microfibers. On the other hand, grass is about 0.5 cm in diameter. When animals walk in the grass field, they are fully surrounded by the grass, but can walk "through." In this case, it appears as animals are embedded in 3-D environment (*right panel*). In analogy to cellular growth in a nanofiber-based scaffold, cells are fully embedded within the scaffold that yet allows cells to migrate/move without much hindrance

fostered a new field of tissue engineering. Attempts have been made to culture cells in 3-D using synthetic polymers or copolymers. However, these synthetic (co)polymers are often processed into microfibers ~10–50 μm in diameter that are similar in size to most cells (~5–20 μm in diameter). Thus, cells attached on microfibers are more or less in a 2-D environment eventhough this is somewhat deviating from 2-D by some curvature imposed by the diameter of the microfibers. Furthermore, the micropores (~10–200 μm cross section) between the microfibers are often ~1,000–10,000-fold greater than the size of biomolecules including vitamins, amino acids, nutrients, proteins or drugs, which as a consequence can quickly diffuse away. In order to culture tissue cells in a truly 3-D microenvironment, the scaffold's fibers and pores should be significantly smaller than cells so that the cells are surrounded by the scaffold, similar to the extracellular environment and native extracellular matrices (Ayad et al. 1998; Kreis et al. 1999; Timpl et al. 1979; Kleinman et al. 1986; Lee et al. 1985; Oliver et al. 1987).

Animal-derived biomaterials (e.g., collagen gels, poly-glycosaminoglycans and Matrigel™) have been used as an alternative to synthetic scaffolds (Kubota et al. 1988; Kleinman et al. 1986; Lee et al. 1985; Oliver et al. 1987; Bissell et al. 2002; Schmeichel and Bissell 2003; Weaver et al. 1995; Zhau et al. 1997; Cukierman et al. 2001; Cukierman et al. 2002). However, while they do have an appropriate scale, they frequently contain residual growth factors, undefined constituents or non-quantified impurities. Due to lack of quality control resulting in lot to lot variations of these materials, it is thus very difficult to conduct a completely controlled study using these biomaterials. Additionally, impurities pose problems if such scaffolds would be


**Fig. 2** Architecture that mimics 3-D cellular architecture and tissue repair. The San Simeon Piccolo Dome in Venice, Italy. Each of the metal rods has a diameter of ~4 cm, 500 times smaller than the size of the dome with a diameter of ~20 m. Each rod also serves as a construction scaffold for building or repairing the dome that is truly embodied in three dimensions (*left panel*). When the repair and construction is completed, the scaffold is removed as shown (*right panel*)

considered for generating cells/tissue used in human therapy. Although researchers are well aware of its limitation, it is one of the few limited choices. Thus, it not only makes difficult to conduct a well-controlled study but also would pose problems if such scaffolds were ever used to grow tissues for human therapies.

Furthermore, after the cells are adapted to the new environment and start to make their own extracellular matrices, the artificial scaffolds that initially helped the cells should be gradually removed through absorption or biodegradation. This is in analogy similar to architectural constructions: after the entity is repaired or constructed, the scaffolds should be removed (Fig. 2).

An ideal 3-D culture system should be fabricated from a synthetic biological material with defined constituents. Thus the molecular designer self-assembling peptide nanofiber scaffolds may be a promising alternative. Figure 3 directly compares the Matrigel with the self-assembling peptide nanofiber scaffold. They have the same scales and similar porosity except Matrigel seems to have many particles/impurities contained within the Matrigel. The peptide nanofibers, however, do not exhibit such morphological impurities and display homogeneous structure (Fig. 3).

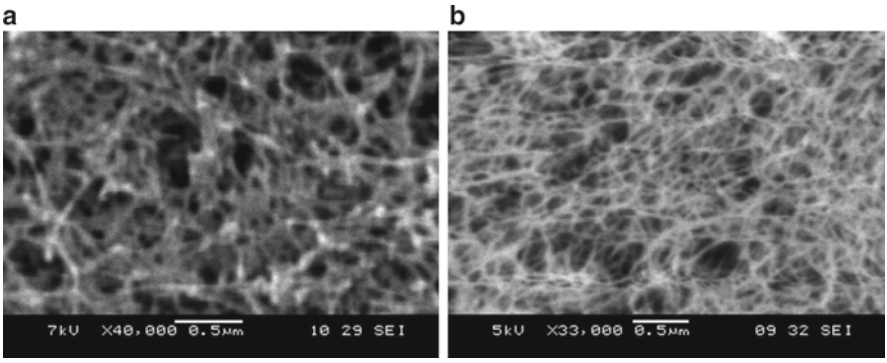


**Fig. 3** Scanning electron microscope images of Matrigel and designed self-assembling peptide nanofiber scaffold. (**a**) Matrigel™, displaying some particulate/impurities. (**b**) The self-assembling peptide RADA16-I nanofiber scaffold lacking particulate appearance and having nanopores (average 5–200 nm). Such nanopores can allow slow diffusion of small molecular drugs (1–2 nm) and proteins (2–10 nm). This is in sharp contrast to many other biopolymer microfiber materials where the micrometer pores permit drugs and proteins to diffuse rather quickly. Scale bars, 0.5 μm

## 4 Ideal Biological Materials

Although there are a number of criteria to fabricate biological scaffolds, the ideal 3-D biological scaffolds should meet several important criteria: (1) the building blocks should be derived from biological sources; (2) basic units should be amenable to design and modification to achieve specific needs; (3) exhibit a controlled rate of material biodegradation; (4) exhibit no cytotoxicity; (5) promote cell–substrate interactions, (6) afford economically scalable and reproducible material production, purification and processing; (7) be readily transportable; (8) be chemically compatible with aqueous solutions and physiological conditions; (9) elicit no or little immune responses and inflammation if used in human therapies; (10) integrate with other materials and tissue in the body.

### *4.1 Self-Assembling Peptide as Biological Material Construction Units*

In the construction industry many other parts of house, such as doors and windows can be prefabricated and then programmed assembled according to architectural plans. If we "shrink" the construction units many orders of magnitude into nanoscale, we can apply similar pre-fabrication principles to construct molecular materials and devices, through molecular programmed molecular assembly, as well as self-assembly. We limit our discussion below to three self-assembling construction units: (1) "Lego peptide" that forms well-ordered nanofiber scaffolds for 3-D cell

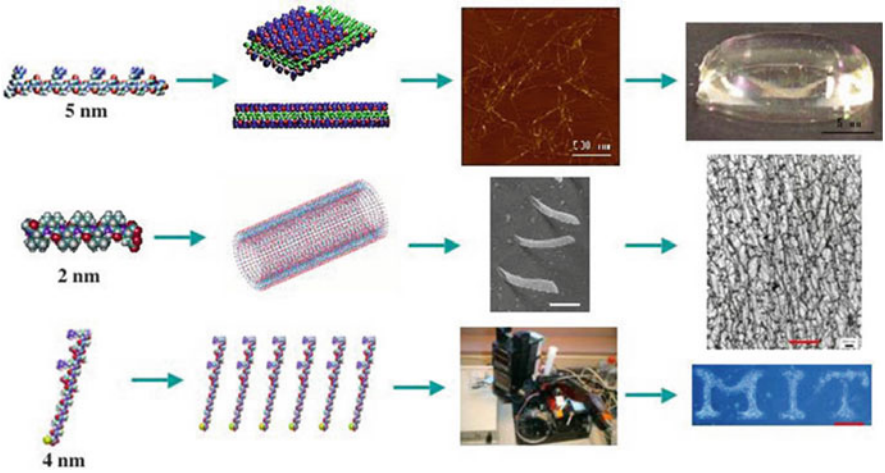


**Fig. 4** Design of various peptide materials. (*Top Panel*) Peptide Lego, also called ionic self-complementary peptide has 16 amino acids, ~5 nm in size, with an alternating polar and nonpolar pattern. They form stable β-strand and β-sheet structures, thus the side chains partition into two sides, one polar and the other nonpolar. They undergo self-assembly to form nanofibers with the nonpolar residues inside (*green*) and positively (*blue*) and negatively (*red*) charged residues form complementary ionic interactions, like a checkerboard. These nanofibers form interwoven matrices that further form a scaffold hydrogel with very high water content, >99.5% water. (*Middle Panel*) Peptide surfactant, ~2 nm in size, which has a distinct head group, either positively or negatively charged, and a hydrophobic tail consisting of six hydrophobic amino acids. They can self-assemble into nanotube and nanovesicles with a diameter of ~30–50 nm (image courtesy Steve Yang and Sylvain Vauthey). These nanotubes go on to form an interconnected network. (*Bottom Panel*) Peptide ink. This type of peptide has three distinct segments: a functional segment where it interacts with other proteins and cells; a linker segment can be flexible or stiff, and it sets the distance from the surface; and an anchor for covalent attachment to the surface. These peptides can be used as ink for an inkjet printer to directly print on a surface, instantly creating any arbitrary pattern, as shown here. Neural cells from rat hippocampal tissue grown on peptide ink substrate with defined pattern. (Images courtesy Sawyer Fuller)

culture and for regenerative medicine; (2) "lipid-like peptides" for drug, protein and gene deliveries as well as for solubilizing and stabilizing membrane proteins; (3) "peptide ink" for surface biological engineering (Fig. 4). These designed construction peptide units are structurally simple and versatile for a wide spectrum of applications as nanobiomaterials and beyond.

### 4.1.1 Discovery of Self-Assembling Peptide Scaffolds

The self-assembling peptide scaffold belongs to a class of biologically inspired materials. The first member, EAK16-II (AEAEAKAKAEAEAKAK), of the family was discovered from a segment in a yeast protein, Zuotin (Zhang et al. 1993), that was characterized as a left-handed Z-DNA binding protein (Zhang et al. 1992).

The scaffolds consist of alternating amino acids that contain 50% charged residues (Zhang et al. 1993, 1994, 1995; Holmes et al. 2000; Caplan et al. 2002; Kisiday et al. 2002; Gelain et al. 2006; Horii et al. 2007; reviewed by Gelain et al. 2007a, b). These peptides are characterized by their periodic repeats of alternating ionic hydrophilic and hydrophobic amino acids with a typical β-sheet structure. Thus, these β-sheet peptides have distinct polar and non-polar surfaces. The self-assembly event creating the peptide scaffold takes place under physiological conditions. They are like gel-sponge in aqueous solution and readily transportable to different environments. Individual fibers are ~10 nm in diameter. A number of additional self-assembling peptides including RADA16-I (AcN-RADARADARADARADA-CNH2) (shown in Fig. 3b) and RADA16-II (AcN-RARADADARARADADA-CNH2), in which arginine and aspartate residues substitute lysine and glutamate, have been designed and characterized for salt-facilitated nanofiber scaffold formation. The alanines form overlap packed hydrophobic interactions in water, a structure that is found in silk fibroin from silkworm and spiders. On the charged sides, both positive and negative charges are packed together through intermolecular ionic interactions in a checkerboard-like manner. In general, these self-assembling peptides form stable β-sheet structures in water, which are stable across a broad range of temperature, wide pH ranges in high concentration of denaturing agent urea and guanidium hydrochloride. The nanofiber density correlates with the concentration of peptide solution and the nanofiber retains extremely high hydration, >99% in water (5–10 mg/ml, w/v) (Fig. 4).

The peptide synthesis method uses conventional mature solid phase peptide synthesis chemistry. Depending on the length of the motifs, high purity of peptides can be produced at a reasonable cost. Since cost of the peptide synthesis has decreased steadily in last few years, it has become more and more affordable.

Many self-assembling peptides that form scaffolds have been reported and the numbers are still expanding (Zhang and Altman 1999; Zhang 2002). The formation of the scaffold and its mechanical properties are influenced by several factors, one of which is the level of hydrophobicity (Marini et al. 2002; Caplan et al. 2002). That is, in addition to the ionic complementary interactions, the extent of the hydrophobic amino acids, Ala, Val, Met, Ile, Leu, Tyr, Phe, Trp (or single letter code, A, V, M, I, L, Y, P, W) can significantly influence the mechanical properties of the scaffolds and the speed of their self-assembly. The higher the content of hydrophobicity, the easier it is for scaffold formation and the better for their mechanical properties (Marini et al. 2002; Caplan et al. 2002; Kisiday et al. 2002).

### 4.1.2 The Molecular Lego Peptides

Molecular-designed “Lego Peptide”, at the nanometer scale, resembles the Lego bricks that have both pegs and holes in a precisely determined manner and can be programmed to assemble in well-formed structures. This class of “Lego peptide” can spontaneously assemble into well-formed nanofibers (Zhang et al. 1993). The first member of the Lego peptide was EAK16-II mentioned above and serendipitously

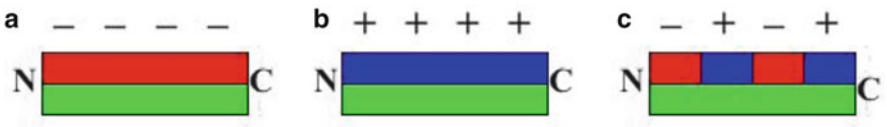


**Fig. 5** Three distinct types of self-assembling "Lego peptides." These peptides have two sides, one hydrophobic (*green*) and another hydrophilic (*red* and *blue*)


**Fig. 6** The designer lipid-like peptides. They have either negatively charged head (*red*) or positively charged head (*blue*) or mixed charged head (*half red* and *half blue* in both sites). The tails can be any hydrophobic amino acids (*green*)

discovered from Zuotin (zuo means left in Chinese, while tin is suffix to assign its peptide nature) (Zhang et al. 1992).

The Lego peptide molecules can undergo self-assembly in aqueous solutions to form well-ordered nanofibers that further associate to form nanofiber scaffolds (Fig. 4). One of them, RADA16-I, is widely used as a designed biological scaffold in contrast to other biologically derived scaffolds from animal collagen and Matrigel, which contain unspecified components in addition to known materials (Fig. 3).

Lego peptides can form stable β-strand and β-sheet structures, thus the side chains partition into two sides, one polar and the other nonpolar (Fig. 5). They undergo self-assembly to form nanofibers with the nonpolar residues inside (green) and positively (blue) and negatively (red) charged residues form complementary ionic interactions, like a checkerboard.

Since these nanofiber scaffolds contain 5–200 nm pores and have extremely high water content (>99.5% or 1–5 mg/ml), they have been used as 3-D cell-culture media. The scaffolds closely mimic the porosity and gross structure of extracellular matrices, allowing cells to reside and migrate in a 3-D environment and molecules, such as growth factors and nutrients, to diffuse in and out very slowly. These peptide scaffolds have been used for 3-D cell culture, controlled cell differentiation, tissue engineering and regenerative medicine applications.

### 4.1.3 Designer Lipid-Like Peptides

The second class of the self-assembling peptide belongs to a lipid-like molecule. These peptides have a hydrophilic head and a hydrophobic tail, much like lipids or detergents. They sequester their hydrophobic tail inside of micelle, vesicles or nanotube structures and their hydrophilic heads expose to water. At least four kinds of molecules can be made, with negative, positive, zwitterionic (±, mixed charge) heads (Vauthey et al. 2002; Santoso et al. 2002; von Maltzahn et al. 2003) (Fig. 6).

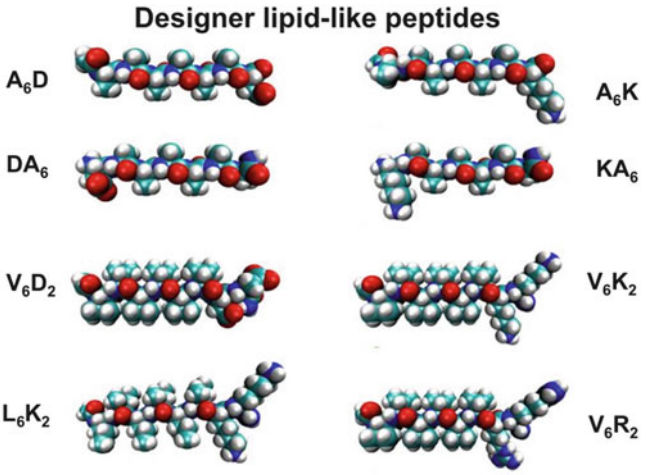


**Fig. 7** Few examples of designer lipid-like peptides. These peptides behave like lipids and surfactants that can undergo self-assembly in water to form well-ordered structures. They can also stabilize diverse membrane proteins and membrane protein complexes. The amino acids are one-letter codes, the number refers to the number of amino acid residues. Color code: *red* oxygen; *blue* nitrogen; *teal* carbon; *white* hydrogen

Several lipid-like peptides have been designed using nature's lipid as a guide. These peptides have a hydrophobic tail with various degrees of hydrophobicity and a hydrophilic head; either negatively charged aspartic and glutamic acids or positively charged lysine or histidine (Fig. 7). These peptide monomers contain 7–8 amino acid residues and have a hydrophilic head composed of aspartic acid and a tail of hydrophobic amino acids, such as alanine, valine or leucine. The length of each peptide is approximately 2 nm, similar to that of biological phospholipids (Vauthey et al. 2002; Santoso et al. 2002; von Maltzahn et al. 2003; Yang and Zhang 2006; Nagai et al. 2007; Yaghmur et al. 2007). The length can also be varied by adding more amino acids, one at a time to a desired length as shown in Fig. 8.

Although individually these lipid-like peptides have completely different composition and sequences, they share a common feature: the hydrophilic heads have 1–2 charged amino acids and the hydrophobic tails have four or more consecutive hydrophobic amino acids. For example, $A_6D$ (ac-AAAAAAD), $V_6D$ (ac-VVVVVVD) peptide has six hydrophobic alanine or valine residues from the N-terminus followed by one negatively charged aspartic acid residues, thus having two negative charges, one from the side chain and the other from the C terminus. In contrast, $V_6K_2$ (ac-VVVVVVKK) or $V_6R_2$ has six valines as the hydrophobic tail followed by two positively charged lysines or arginines as the hydrophilic head (Vauthey et al. 2002; Santoso et al. 2002; von Maltzahn et al. 2003; Yang and Zhang 2006; Nagai et al. 2007; Yaghmur et al. 2007).

Since these lipid-like peptides are not directly relevant to tissue regeneration, we will not elaborate on them further. Their applications in material sciences sprout

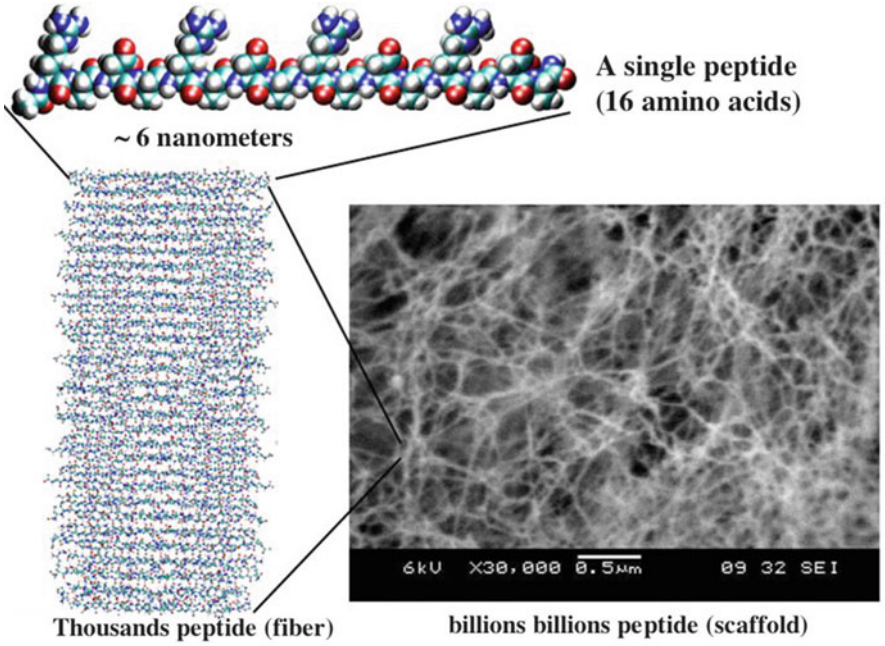


**Fig. 8** Self-assembling peptide RADA16-I nanofiber scaffold hydrogel. (*Top*) Molecular model of RADA16-I. (*Left*) Molecular model of a single RADA16-I nanofiber with its dimensions being ~6 nm long, 1.3 nm wide and 0.8 nm thick. Many individual peptides self-assemble into a nanofiber. (*Right*) SEM images of RADA16-I nanofiber scaffold. Scale bar, 0.5 μm

from their ability to stabilize a number of membrane proteins and membrane protein complexes (Kiley et al. 2005; Yeh et al. 2005; Zhao et al. 2006). Interested readers can consult the original reports and a recent summary (Zhao and Zhang 2006).

## *4.2 Self-Assembling Peptide Nanofiber Scaffolds*

A single molecule of the ionic self-complementary peptide RADA16-I is shown in Fig. 8. Millions of peptide molecules spontaneously undergo self-assembly into individual nanofibers that further form the scaffold (Fig. 8). Between the nanofibers, there are numerous nanopores. The nanopores range from a few to a few hundred nanometers. Such structuring is similarly sized as most biomolecules and allows only slow diffusion of molecules within the scaffold and can be used to establish a molecular gradient. Figure 9 shows the individual nanofibers ranging from a few hundred nanometers to a few microns. Peptide samples in aqueous solution using an atomic force microscopy (AFM) examination display nanofibers (Fig. 9b–d), which at high resolution appear to have distinct layers in some of their segments (Fig. 9d)

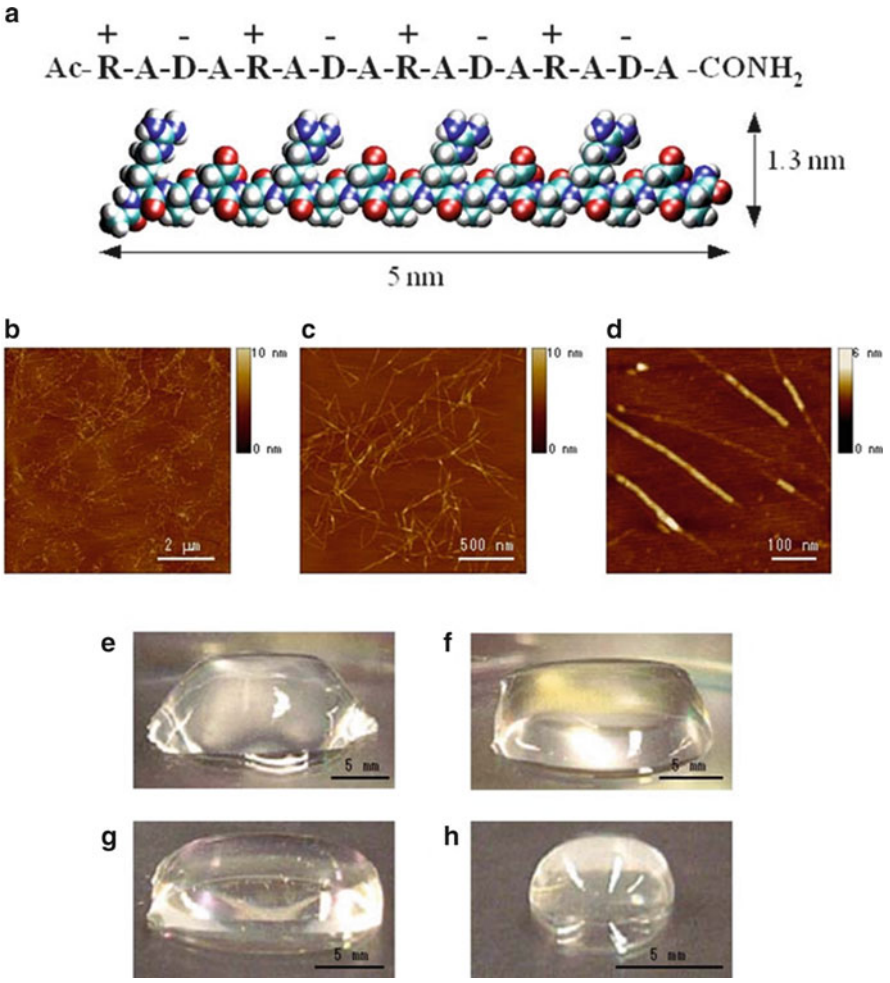


**Fig. 9** Peptide RADA16-I. (**a**) Amino acid sequence and molecular model of RADA16-I (~5 nm long, 1.3 nm wide and 0.8 nm thick). (**b–d**) AFM images of RADA16-I nanofiber scaffold. Image size, (**b**) 8×8 μm, (**c**) 2×2 μm, and (**d**) 0.5×0.5 μm. Note variability in height by ~1.3 nm of different segments within individual nanofiber suggesting its double-layered structure (**d**). (**e–h**) Photographs of RADA16-I hydrogel at various condition, (**e**) 0.5 wt.% (pH 7.5), (**f**) 0.1 wt.% (pH 7.5, Tris.HCl), (**g**) 0.1 wt.% (pH 7.5, PBS) before sonication, (**h**) reassembled RADA16-I hydrogel after four times of sonication, respectively

as distinct increase in height of about 1.3–1.5 nm can be seen; this height corresponds to the addition of a single thickness of a peptide. Figure 9e–h shows the peptide scaffold hydrogel formation at various concentrations [0.6–3 mM, or 1–5 mg/ml (w/v)] and water content (99.5–99.9%) (Yokoi et al. 2005). The scaffold hydrogel is completely transparent, which is a very important requirement for accurate image collections for uses in 3-D tissue cell cultures.

## *4.3 Dynamic Reassembly of Self-Assembling Peptides*

The self-assembling process is reversible and dynamic (Fig. 10). Since these peptides are short and simple, numerous individual peptides can be readily self-organized through the weak interactions including hydrogen bonds, ionic bonds, hydrophobic and van der Waals interactions as well as water-mediated hydrogen bond formations. Once self-assembled, nanofibers can be broken mechanically with sonication (Yokoi et al. 2005) and can undergo dynamic self-reassembly repeatedly, in a process that resembles a self-healing process (Fig. 10). Since the driving energy of their assembly in water is governed by variety of interactions, this phenomenon can be further exploited for production and fabrication of many variants of such materials.

Unlike processed polymer microfibers in which the fragments of polymers cannot readily undergo reassembly without addition of catalysts or through material processing, the supramolecular self-assembly and reassembly event we uncovered here is likely to be wide spread in many unrelated fibrous biological materials where there are numerous weak interactions involved. Self-assembly and reassembly are a very important property for fabricating novel materials, and it is necessary to fully understand its detailed process in order to design better biological materials. We unequivocally demonstrated the reassembly process since we used the same peptide solutions from a single experimental test tube throughout the four repeated experimental cycles. This remarkable and rapid, initiated within minutes and fully accomplished within ~1–2 with hours, reassembly is interesting because there may be a little nucleation for regrowth of the nanofiber from the addition of monomers that could only be produced during sonication. It is plausible that a large population of the sonicated nanofiber fragments contains many overlap cohesive ends due to un-disrupted alanine hydrophobic side that may quickly find each other (Fig. 9d). The situation is analogous and commonly found in sonicated and enzymatic digested DNA fragments.

### 4.3.1 Kinetics of Nanofiber Reassembly and a Plausible Reassembly Process

The reassembly kinetics is a function of time. Perhaps, similar to DNA reassembly, the reassembly of peptides largely depends on the concentrations of the short complementary fragments. In this case, the fragments are the sonicated peptide nanofibers with possible presence of sonicated monomers.

In order to understand the dynamic reassembly, we proposed a plausible sliding diffusion molecular model to interpret these observations of reassembly of the self-assembling RADA16-I peptides (Fig. 11). Unlike the left-handed helical structures observed in KFE8 (Marini et al. 2002), a different self-assembling peptide, no helical structures were observed for RADA16-I using AFM and transmission electron microscopy (TEM) (Holmes et al. 2000; Gelain et al. 2006).

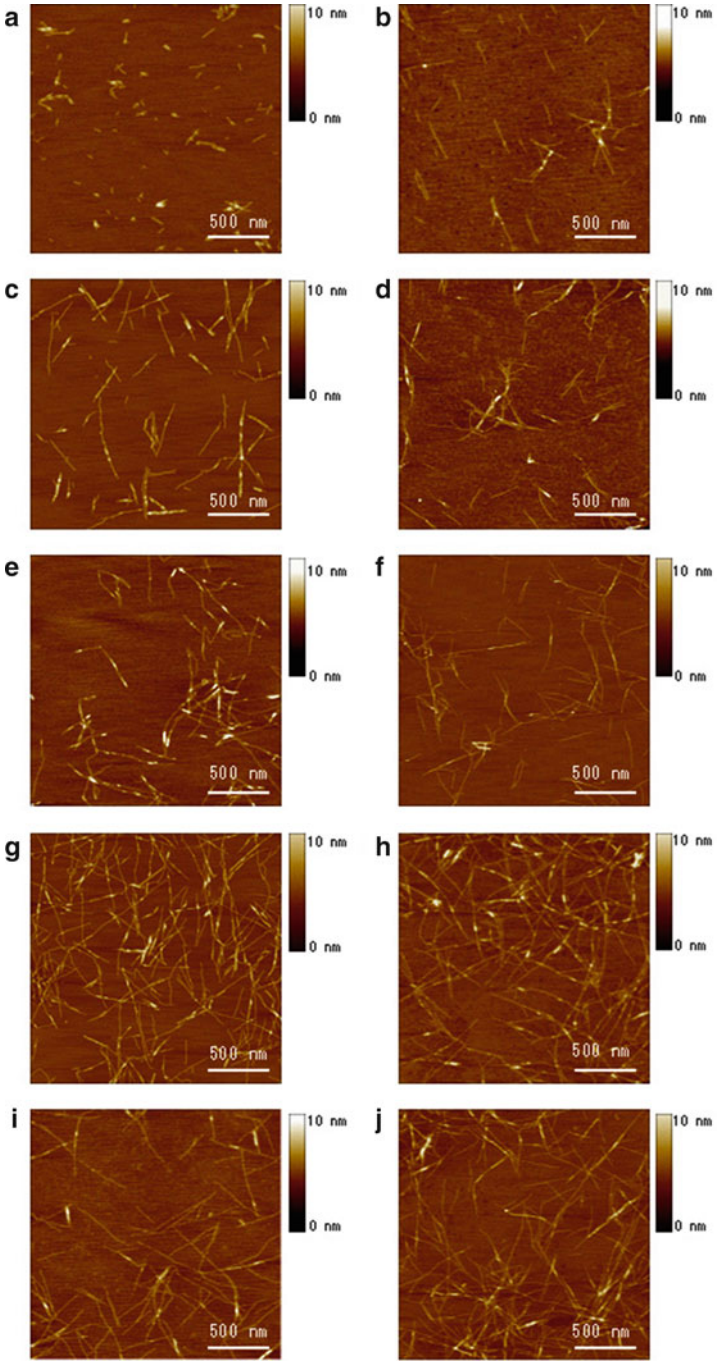


**Fig. 10** AFM images of RADA16-I nanofibers at various time points after sonication. The observations were made using AFM immediately after sample preparation. (**a**) 1 min; (**b**) 2 min; (**c**) 4 min; (**d**) 8 min; (**e**) 16 min; (**f**) 32 min; (**g**) 64 min; (**h**) 2 h; (**i**) 4 h; (**j**) 24 h after sonication. Note the elongation and reassembly of the peptide nanofibers over time. By ~1–2 h, these self-assembling peptide nanofibers have nearly fully reassembled

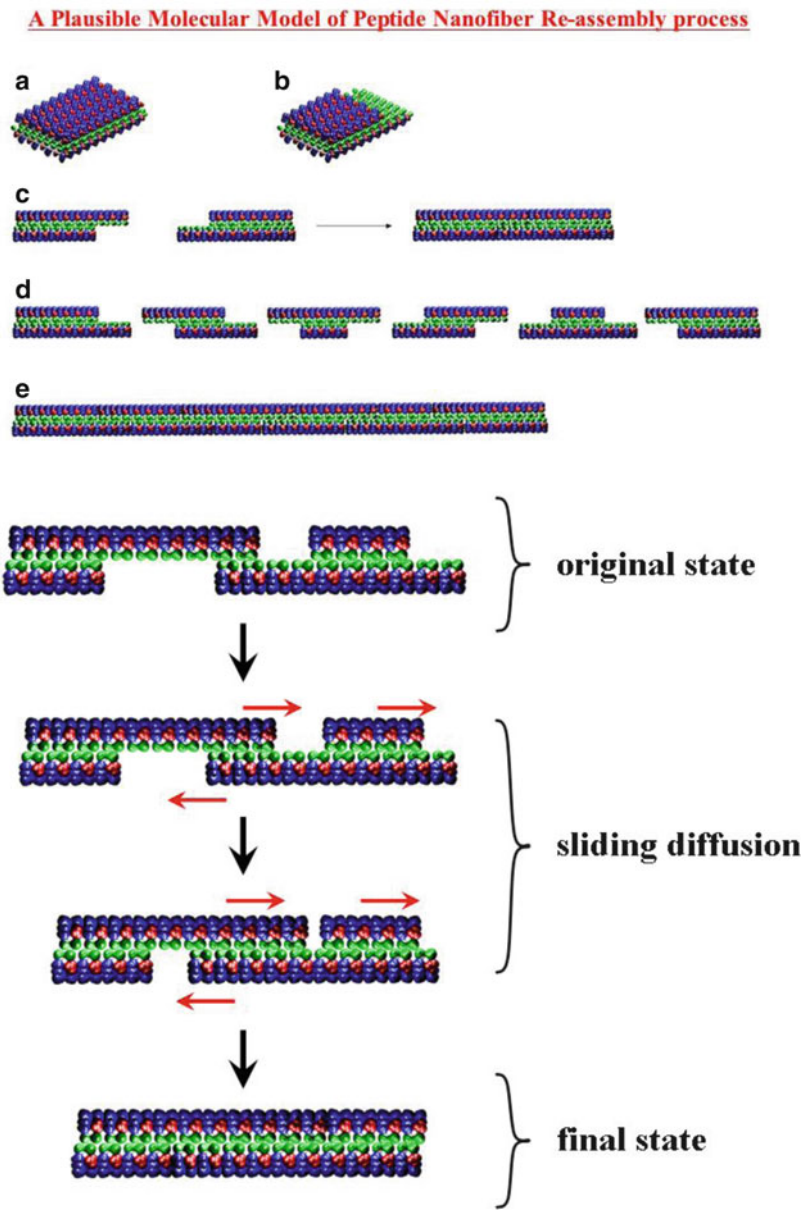
A Plausible Molecular Model of Peptide Nanofiber Re-assembly process
a
b
c
d
e
original state
sliding diffusion
final state

RADA16-I peptide can form stable β-sheet structure in water (Fig. 11). Thus, they not only form the intermolecular hydrogen bonding on the peptide backbones but they also have two distinctive sides, one hydrophobic with array of overlapping alanines (Fig. 11, green color sandwiched inside), similar as found in silk fibroin or spider silk assemblies (Pauling 1960). The other side of the backbones has negatively charged (−) aspartic acids represented as red and positively charged (+) arginines represented as blue. The alanines form packed hydrophobic interactions in water; during sonication, the hydrophobic interaction could be disrupted mechanically. However, these hydrophobic cohesive ends could find each other quickly in water since the exposure of hydrophobic alanine arrays to water is energetically unfavorable. Since the hydrophobic alanines interaction is non-specific, they can slide diffuse along the nanofiber. The same sliding diffusion phenomenon was also observed in nucleic acids where polyA and polyU form complementary base pairings that can slide diffuse along the chains (Rich and Davies 1956; Felsenfeld et al. 1957). If, however, the bases are heterogonous, containing G, A, T, C, the bases cannot undergo sliding diffusion. Likewise, if the hydrophobic side of the peptides does not always contain alanine, such as valine and isoleucine, it would become more difficult for sliding diffusion to occur due to structure constraint.

On the charged side, both positive and negative charges are packed together through intermolecular ionic interactions in a checkerboard manner (looking from the top). Likewise, the collectively complementary positive and negative ionic interactions may also facilitate the reassembly. Similar to restriction-digested DNA fragments, these nanofiber fragments could form various assemblies: blunt, semi-protruding and protruding ends. The fragments with semi-protruding and various protruding ends as well as blunt ends can reassemble readily through hydrophobic and ionic interactions.

**Fig. 11** A proposed molecular sliding diffusion model for dynamic reassembly of self-assembling RADA16-I peptides. When the peptides form stable β-sheets in water, they form intermolecular hydrogen bonds along the peptide backbones. The β-sheets have two distinctive sides, one hydrophobic with an array of alanines and the other with negatively charged aspartic acids and positively charged arginines. These peptides form anti-parallel β-sheet structures. The alanines form overlap packed hydrophobic interactions in water. On the charged sides, both positive and negative charges are packed together through intermolecular ionic interactions in a checkerboard-like manner. These nanofiber fragments can form various assemblies similar to restriction-digested DNA fragments: (**a**) blunt ends; (**b**) semi-protruding ends; (**c**) These fragments with protruding ends could reassemble readily through hydrophobic interactions; (**d**) The fragments with semi-protruding and various protruding ends; (**e**) These fragments can reassemble readily. (*Bottom*) A proposed molecular sliding diffusion model for dynamic reassembly of self-assembling a single peptide nanofiber consisting thousands of individual peptides. When the fragments of nanofiber first meet, the hydrophobic sides may not fit perfectly but with gaps (original state). However, the non-specific hydrophobic interactions permit the nanofiber to slide diffusion (sliding diffusion) along the fiber in either direction that minimizes the exposure of hydrophobic alanines and eventually fill the gaps (final state). For clarity, these β-sheets are not presented as twisted strands. Color code: *green* alanines; *red* negatively charged aspartic acids; *blue* positively charged arginines

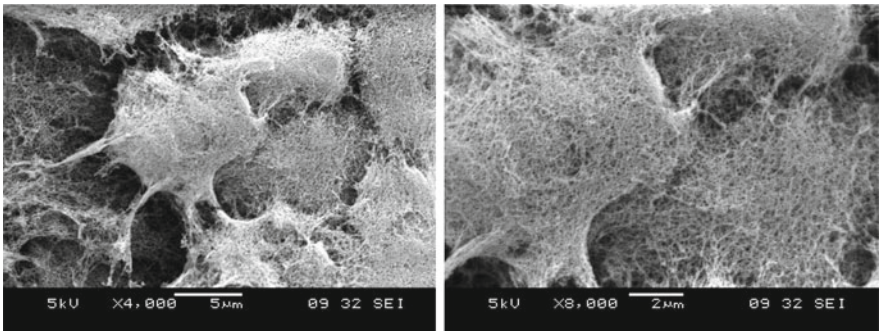


**Fig. 12** Cluster of cells are fully embedded in the self-assembling peptide nanofiber scaffold. The scales of the nanofibers are on the similar scale as the native extracellular matrices. Such 3-D cell clusters are nearly impossible to form in the 2-D culture systems

## *4.4 Self-Assembling Peptides Nanofiber Scaffold 3-D Cell Culture*

The importance of nanoscale becomes obvious in 3-D cell culture. It is clearly visible in the scanning electron microcopy (SEM) images that the cells embed in the self-assembling peptide nanofiber biological scaffolds in the truly 3-D culture (Fig. 12). Here, the cells and cell clusters intimately interact with the extracellular matrix that the cells make on their own. Since the scaffolds are made mostly of water, ~99% water at 1% peptide solid, cells can migrate freely without hindrance.

These new self-assembling peptide nanofiber biological scaffolds have become increasingly important not only in studying spatial behaviors of cells, but also in developing approaches for a wide range of innovative medical technologies including regenerative medicine (Fig. 13). One example is the use of the peptide scaffolds to support neurite growth and differentiation, neural stem cell differentiation, cardiac myocytes, bone and cartilage cell cultures. The peptide scaffolds from RADA16-I and RADA16-II form nanofiber scaffold in physiological solutions that stimulated extensive rat neurite outgrowth, and active synapses formation on the peptide scaffold was successfully achieved (Holmes et al. 2000).

## *4.5 Designer Peptides Scaffold 3-D Cell Cultures*

A variety of mammalian cells have been cultured on designer self-assembling peptide nanofiber scaffolds (Table 1). In a recent work we directly and systematically compared neural stem cell adhesion and differentiation on self-assembling RADA16-I scaffolds with other natural-based substrates including laminin, Collagen I, fibronectin and some of the most commonly used synthetic biomaterials in tissue

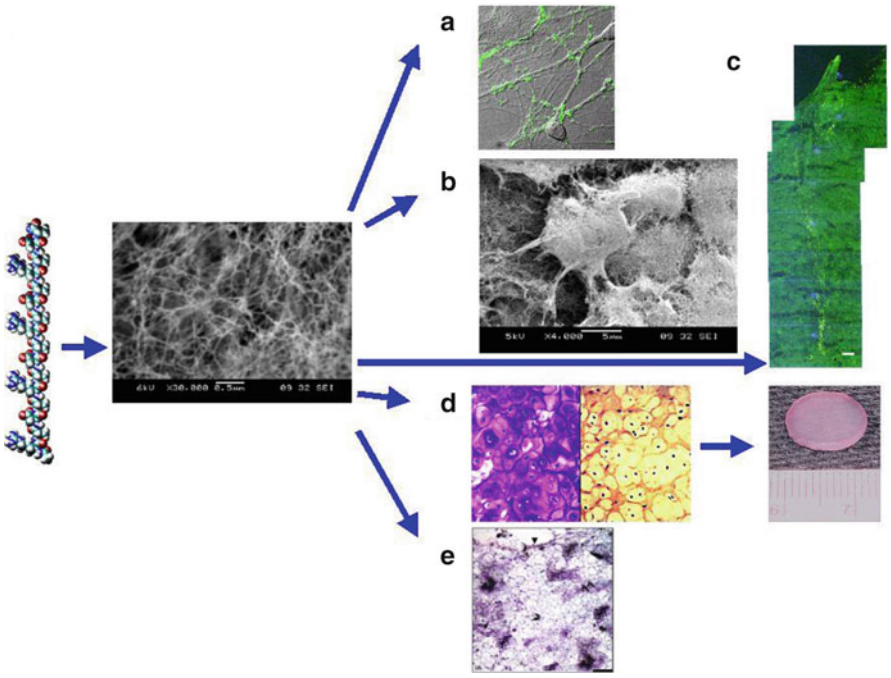


**Fig. 13** From designer self-assembling peptides to nanofibers to scaffolds to tissues. (**a**) Active synapses on the peptide surface. Primary rat hippocampal neurons form active synapses on peptide scaffolds. The confocal images shown in bright discrete *green dot* labeling are indicative of synaptically active sites after incubation of neurons with the fluorescent lipophilic probe FM1-43. The active synapses on the peptide scaffold are fully functional, indicating that the peptide scaffold is a permissible material for neurite outgrowth and active synapse formation. (**b**) Adult mouse neural stem cells embedded in 3-D scaffold. (**c**) Brain damage repair in hamster. The peptide scaffold was injected into the optical nerve area of brain that was first severed with a knife. The cut was sealed by the migrating cells after 2 days. A great number of neurons form synapses (image courtesy of Rutledge Ellis-Behnke). (**d**) Chondrocytes in the peptide KLD12 (KLDLKLDLKLDL) scaffold and cartilage formation. The trypan *blue-stained* chondrocytes show abundant glycosaminoglycan production (*left panel*), while antibody to type II collagen demonstrates abundant Type II collagen production (*right panel*). A piece of pre-molded cartilage with encapsulated chondrocytes in the peptide nanofiber scaffold. The cartilage formed over a 3–4 week period after the initial seeding of the chondrocytes (image courtesy of John Kisiday). (**e**) Von Kossa staining showing transverse sections of primary osteoblast cells on HA-PHP-RADA16-I self-assembling peptide nanofiber scaffold. Scale bar = 0.1 mm. The intensely stained *black areas* represent bone nodules forming (image courtesy of Maria Bokhari et al. 2005)

engineering, such as poly- (DL-lactic acid), poly- (lactide-co-glycolide acid) and poly- (capro-lactone acid) (Gelain et al. 2007a, b). While natural-derived substrates showed the best performances, RADA16-I scaffold coaxed neural stem cell differentiation and survival to a similar degree of the other synthetic biomaterials.

Although self-assembling peptides are promising scaffolds, they show no specific cell interaction because their sequences are not naturally found in living

**Table 1** A variety of tissue cells cultured on the designer self-assembling peptide nanofiber scaffolds

| | |
|---|---|
| Chicken embryo fibroblast | Bovine calf and adult chondrocytes |
| Mouse fibroblast | Bovine endothelial cells |
| Mouse embryonic stem cells | Mouse adult neural stem cells |
| Mouse cerebellum granule cells | Mouse and rat hippocampal cells |
| Mouse mesenchymal stem cells | Mouse cardiac myocytes |
| Rat adult liver progenitor cells | Rat liver hepatocytes |
| Rat pheochromocytoma | Rat cardiac myocytes |
| Rat neural stem cells | Rat hippocampal neural tissue slice |
| Bovine osteoblasts | Bovine endothelium cells |
| Chinese hamster ovary | Hamster pancreas cells |
| Horse bone marrow | Rat keratinocytes |
| Human cervical carcinoma | Human osteosarcoma |
| Human hepato-cellular carcinoma | Human neuroblastoma |
| Human embryonic kidney | Human Hodgkin's lymphoma |
| Human epidermal keratinocytes | Human foreskin fibroblast |
| Human neural stem cells | Human aortic endothelial cells |

*Note*: These cells include stable cell lines, primary isolated cells from animals, progenitor and adult stem cells. These cells are known to be cultured in various laboratories. Since this compilation, the peptide scaffolds have been commercialized and many more cell types may have been cultured on them

systems. The next step is to directly couple biologically active and functional peptide motifs to generate the second generation of designer scaffolds that would significantly improve their interactions with cells and tissues.

The simplest way to incorporate the functional motifs is to directly synthesize them by extending the motifs on to the self-assembling peptides themselves (Fig. 14). The functional motifs are on the C-termini, since peptide synthesis starts from C-termini to avoid deletion during synthesis. Usually a spacer comprising two glycine residues is added to guarantee a flexible and correct exposure of the motifs to cell surface receptors. Different functional motifs in various ratios can be incorporated in the same scaffold. Upon exposure to solution with neutral pH, the functionalized sequences self-assemble leaving the added motifs flagging on both sides of each nanofiber (Fig. 14). These nanofibers with functional motifs take part in the overall scaffold thus giving microenvironments functionalized with specific biological stimuli (Fig. 14).

The self-assembling peptide scaffolds with functional motifs can be commercially produced with a reasonable cost. Thus, this method can be readily adopted for widespread uses including study how cell interact with their local- and microenvironments, cell migrations in 3-D, tumor and cancer cells' interactions with normal cells, cell process and neurite extensions, cell-based drug test assays and other diverse applications.

We have produced different designer peptides from a variety of functional motifs with different lengths (Gelain et al. 2006; Horii et al. 2007). We showed that the addition of motifs to the self-assembling peptide RADA16-I did not inhibit

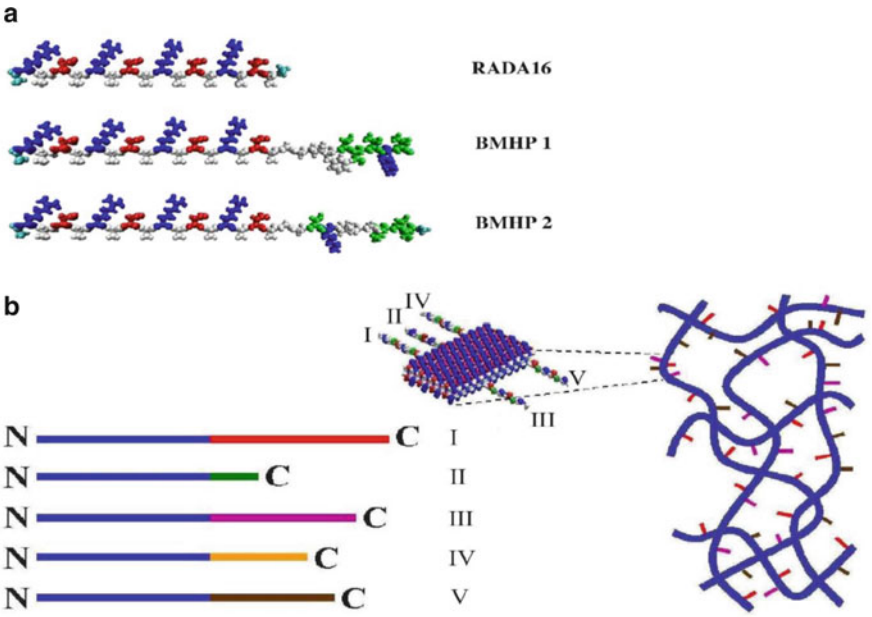


**Fig. 14** Molecular and schematic models of the designer peptides and of the scaffolds. (**a**) Molecular models of RADA16, RADA16-Bone Marrow Homing Peptide 1 (BMHP1) and RADA16-Bone Marrow Homing Peptide 2 (BMHP2). RADA16 is an alternating16-residue peptide with basic arginine (*blue*), hydrophobic alanine (*white*) and aspartic acid (*red*). These peptides self-assemble once exposed to physiological pH solutions or salt. The alanines of the RADA16 providing hydrophobic interaction are on one side of the peptide, and the arginines and aspartates form complementary ionic bonds on the other. The BMHP1 and BMHP2 motifs were directly extended from RADA16 with two glycine spacers and are composed of a lysine (*blue*), serine and threonine (*green*) and different hydrophobic (*white*) residues. Neutral polar residues are drawn in *green*. (**b**) Schematic models of several different functional motifs (different *colored bars*) could be extended from RADA16 (*blue bars*) in order to design different peptides (I, II, III, IV and V). They can be combined in different ratios. A schematic model of a self-assembling nanofiber scaffold with combinatorial motifs carrying different biological functions is shown

self-assembling properties and nanofiber formations through mixing the modified peptides with the original RADA16-I. Although their nanofiber structures appear to be indistinguishable from the RADA16-I scaffold, the appended functional motifs significantly influenced cell behaviors.

Using the designer self-assembling peptide nanofiber system, every ingredient of the scaffold can be defined and combined with various functionalities including the soluble factors. This is in sharp contrast with 2-D systems where cells attach and spread only on the planar surface; cells residing in a 3-D environment can interact with their extracellular matrix receptors to functional ligands appended to the peptide scaffolds. It is possible that higher tissue architectures with multiple cell types, rather than monolayers, could be constructed using these designer 3-D self-assembling peptide nanofiber scaffolds.

In our search for additional functional motifs, we found that a class of bone marrow homing peptides (BMHPs) (Gelain et al. 2006, 2007a, b) is one of the most promising active motifs for stimulating adult mouse neural stem cells (NSC) adhesion and differentiation. Likewise, we also found a newly designed two units of cell adhesion motif that enhanced bone cell differentiation and 3-D migration (Horii et al. 2007). These observations suggest a new class of designer self-assembling peptides for 3-D cell biology studies.

#### 4.5.1 Designer Peptide Scaffolds for Bone Cells and 3-D Migration

The designer self-assembling peptide nanofiber scaffolds has been shown to be an excellent biological material for 3-D cell cultures and capable to stimulate cell migration into the scaffold as well for repairing tissue defects in animals. We developed several peptide nanofiber scaffolds designed specifically for osteoblasts (Horii et al. 2007). We designed one of the pure self-assembling peptide scaffolds RADA16-I through direct coupling to short biologically active motifs. The motifs included osteogenic growth peptide ALK (ALKRQGRTLYGF) bone-cell secreted-signal peptide, osteopontin cell adhesion motif DGR (DGRGDSVAYG) and 2-unit RGD binding sequence PGR (PRGDSGYRGDS). We made the new peptide scaffolds by mixing the pure RADA16-I and designer peptide solutions, and we examined the molecular integration of the mixed nanofiber scaffolds using AFM. Compared to pure RADA16-I scaffold, we found that these designer peptide scaffolds significantly promoted mouse pre-osteoblast MC3T3-E1 cell proliferation. Moreover, alkaline phosphatase (ALP) activity and osteocalcin secretion, which are early and late markers for osteoblastic differentiation, were also significantly increased. We demonstrated that the designer, self-assembling peptide scaffolds promoted the proliferation and osteogenic differentiation of MC3T3-E1. Under the identical culture medium condition, confocal images unequivocally demonstrated that the designer PRG peptide scaffold stimulated cell migration into the 3-D scaffold (Fig. 15) (Horii et al. 2007). Without the modified motif, cells did not migrate into 3-D.

### *4.6 Why Designer Self-Assembling Peptide Scaffolds?*

One may ask why one should choose designer self-assembling peptide scaffolds while there are a large number of biomaterials on the market and some have already been approved by the U.S Food and Drug Administration (FDA). The advantage of using the designer peptide nanofiber scaffolds is severalfold. (1) One can readily modify the designer peptides at the single amino acid level at will, inexpensively and quickly. This level of modification is impossible with Matrigel and other polymer scaffolds. (2) Unlike Matrigel, which contains unknown ingredients and quality that varies from batch to batch, the designer self-assembling peptide scaffolds belong to a class of synthetic biological scaffolds that contains pure components and every ingredient is completely defined. (3) Because these designer peptide scaffolds are

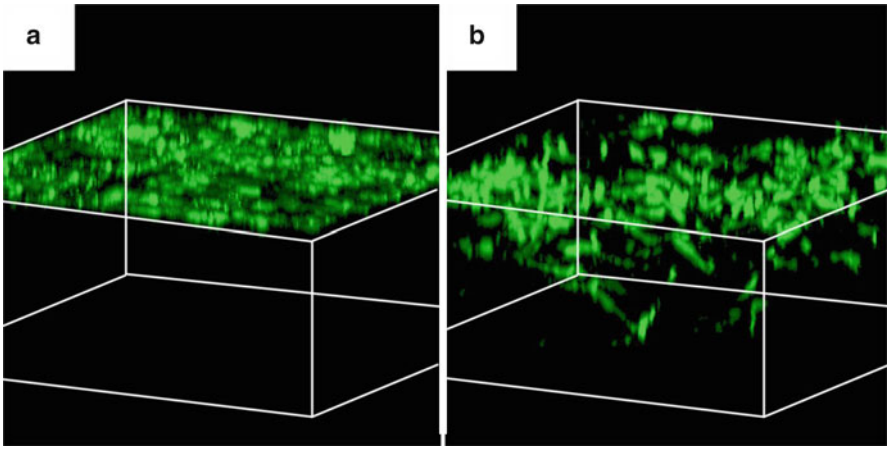


**Fig. 15** Reconstructed image of 3-D confocal microscope image of culturing PRG scaffolds. The vertical depth is ~400 μm. (**a**) 10% PRG scaffold where the cells stayed on the surface of the scaffold. (**b**) 70% PRG scaffold where the cells migrated into the scaffold. There is a drastic cell migration into the scaffold with higher concentration of the PRG motif

well defined using the known motifs, it can be used to study controlled gene expression or cell signaling process. Thus these new designer nanofiber scaffolds proved to be promising tools to study cell signal pathways in a selective way not possible with any substrates including Matrigel and collagen gels, which result in confusing cell signaling activation. (4) The initiation of the self-assembly process is through change of ionic strength at the physiological conditions without temperature influence. This is again unlike collagen gels, for which the gelation is through change of temperature that can sometimes induce unknown biological process including cold or heat shocks. (5) These scaffolds provide the opportunity to incorporate a number of different functional motifs and their combinations to study cell behavior in a well-defined ECM-analog microenvironment, not only without any chemical cross-link reactions but also fully bio-reabsorbable scaffolds. It should be noted that various animals, including mice, rats, hamsters, rabbits, goats, monkey, pigs and horses, have been exposed to peptide nanofiber scaffolds. The tests conducted in different academic laboratories, commercial laboratories, as well as biomaterials and medical device companies around the world indicate that peptide nanofiber scaffolds appeared to be harmless to animal health.

## 5 Beyond 3-D Cell Cultures

Researchers in neuroscience have a strong desire to study neural cell behaviors in 3-D and to fully understand their connections and information transmission (Edelman and Keefer 2005). Since the building blocks of designer peptide scaffolds

are natural L-amino acids, the RADA16-I has been shown not to elicit noticeable immune response, nor inflammatory reactions in animals (Zhang et al. 2005; Davis et al. 2005; Ellis-Behnke et al. 2006 a, b), the degraded products can be reused by the body, they may also be useful as a bio-reabsorbable scaffold for neural repair and neuroengineering to alleviate and to treat a number of neuro-trauma and neuro-degeneration diseases.

In a recent work led by Richard Lee, mouse embryonic stem cells were suspended in RADA16-II peptide scaffold solutions and injected in the myocardium of 10-weeks-old mice (Davis et al. 2005). In that study it has been demonstrated that self-assembling peptides can be injected into the myocardium to create 3-D microenvironment. After 7, 14 and 28 days these microenvironments recruit both endogenous endothelial and smooth muscle cells, and exogenously injected cells survive in the microenvironments: self-assembling peptides can thus create injectable microenvironments that promote vascularization.

In addition Lee's group also developed an appealing drug delivery strategy by using a biotinylated version of RADA-II to demonstrate a slow release of Insulin-like growth factor 1 (IGF-1) in infarctuated rat myocardia (Davis et al. 2006). The biotin sandwich strategy allowed binding of IGF-1 and did not prevent self-assembly of the peptides into nanofibers within the myocardium. In conjunction with cardiomyocytes transplantation the strategy showed that cell therapy with IGF-1 delivery by biotinylated nanofibers significantly improved systolic function after experimental myocardial infarction.

Ellis-Behnke and colleagues showed that self-assembling peptide material is a promising scaffold for neural regeneration medicine (Ellis-Behnke et al. 2006 a, b). In vivo application to brain wounds was carried out using postnatal day-2 Syrian hamster pups. The optic tract within the superior colliculus (SC) was completely severed with a deep knife wound, extending at least 1 mm below the surface. At surgery, ten animals were treated by injection into the wound with 10–30 μl of 1% RADA16-I in 99% water (w/v). Control animals with the same brain lesion included 3 with isotonic saline injection (10 μl), and numerous additional cases, including 10 in which the dye Congo red was added into the peptide scaffold, and 27 earlier animals with knife cuts and no injection surviving 6–9 days. Animals were sacrificed at 1, 3, 6, 30 and 60 days for brain examinations. Histological specimen examinations revealed that only in the peptide scaffold-injected animals, but not in untreated animals, the brain tissue appears to have reconnected itself together in all survival times. Additionally, axons labeled from their retinal origin with a tracer molecule were found to have grown beyond the tissue bridge, reinnervating the SC caudal to the lesion. Most importantly, functional tests proved a significant restoration of visual function in all peptide scaffold-treated animals.

Ellis-Behnke and colleagues during the brain surgery experiments found that the peptide nanofiber scaffold hydrogel could also stop bleeding in less than 15 s (Ellis-Behnke et al. 2007). This is unlikely to be the conventional blood clogging mechanism because it takes place so rapidly. The molecular mechanism of speedy stopping bleeding still remains to be uncovered. It is plausible that the nanofibers self-assembled

at the site quickly self-assembled into a dense mesh nanofiber network sponge that instantly blocked the rushing of the liquid. It may be perhaps nano-mechanics rather than biochemistry.

The development of new biological materials, particularly those biologically inspired nanoscale scaffolds mimicking in vivo environment, that serve as permissive substrates for cell growth, differentiation and biological function is an actively pursued area, which in turn could significantly advance regenerative medicine. These materials will be useful not only for further understanding of cell biology in 3-D environment but also for advancing medical technology, regenerative biology and medicine.

**Acknowledgments** We gratefully acknowledge the supports by grants from Olympus Corp., Japan; Menicon, Ltd, Japan and fellowship to FG from Fondazione Centro San Raffaele del Monte Tabor, Milan, Italy.

## References

Atala A, Lanza R (2002) Methods of Tissue Engineering Academic Press.

Ayad S B-HR, Humphries M, Kadler K, Shuttleworth A (1998) The Extracellular Matrix Factsbook. 2nd Ed Academic Press.

Bissell MJ (1981) The differentiated state of normal and malignant cells or how to define a "normal" cell in culture. Int Rev Cytol 70:27–100.

Bissell MJ, Radisky DC, Rizki A, Weaver VM, Petersen OW (2002) The organizing principle: microenvironmental influences in the normal and malignant breast. Differentiation 70: 537–546.

Bokhari MA, Akay G, Zhang S, Birch MA (2005) The enhancement of osteoblast growth and differentiation in vitro on a peptide hydrogel-polyHIPE polymer hybrid material. Biomaterials 26:5198–5208.

Caplan M, Schwartzfarb E, Zhang S, Kamm R, Lauffenburger D (2002) Control of self-assembling oligopeptide matrix formation through systematic variation of amino acid sequence. Biomaterials 23:219–227.

Cukierman E, Pankov R, Yamada KM (2002) Cell interactions with three-dimensional matrices. Curr Opin Cell Biol 14:633–639.

Cukierman E, Pankov R, Stevens D, Yamada K (2001) Taking cell-matrix adhesions to the third dimension. Science 294:1708–1712.

Davis ME, Motion JP, Narmoneva DA, Takahashi T, Hakuno D, Kamm RD, Zhang S, Lee RT (2005) Injectable self-assembling peptide nanofibers create intramyocardial microenvironments for endothelial cells. Circulation 111:442–450.

Davis ME, Hsieh PC, Takahashi T, Song Q, Zhang S, Kamm RD, Grodzinsky AJ, Anversa P, Lee RT (2006) Local myocardial insulin-like growth factor 1 (IGF-1) delivery with biotinylated peptide nanofibers improves cell therapy for myocardial infarction. Proc Natl Acad Sci U S A 103:8155–8160.

Edelman DB, Keefer EW (2005) A cultural renaissance: in vitro cell biology embraces three-dimensional context. Exp Neurol 192:1–6.

Ellis-Behnke RG, So K-F, Zhang S (2006) Molecular repair of the brain using self-assembling peptides. Chemistry Today 24:42–45.

Ellis-Behnke RG, Liang YX, Tay DKC, Kau PWF, Schneider GE, Zhang S, Wu W, So K.-F (2006) Nano hemostat solution: immediate hemostasis at the nanoscale. Nanomedicine. Nanotechnology, Biology & Medicine 2:207–215.

Ellis-Behnke RG, Liang YX, You SW, Tay DK, Zhang S, So KF, Schneider GE (2006a) Nano neuro knitting: peptide nanofiber scaffold for brain repair and axon regeneration with functional return of vision. Proc Natl Acad Sci U S A 103:5054–5059.

Ellis-Behnke RG, Liang YX, Tay DK, Kau PW, Schneider GE, Zhang S, Wu W, So KF (2006b) Nano hemostat solution: immediate hemostasis at the nanoscale. Nanomedicine 2:207–215.

Felsenfeld G, Davies DR, Rich A (1957) Formation of a three-stranded polynucleotide molecule. J Am Chem Soc 79:2023–2024.

Gelain F, Horii A, Zhang S (2007a) Designer self-assembling peptide scaffolds for 3-d tissue cell cultures and regenerative medicine. Macromol Biosci 7:544–551.

Gelain F, Bottai D, Vescovi A, Zhang S (2006) Designer self-assembling peptide nanofiber scaffolds for adult mouse neural stem cell 3-dimensional cultures. PLoS One 1:e119.

Gelain F, Lomander A, Vescovi AL, Zhang S (2007b) Systematic studies of a self-assembling peptide nanofiber scaffold with other scaffolds. J Nanosci Nanotechnol 7:424–434.

Hoffman AS (2002) Hydrogels for biomedical applications. Adv Drug Deliv Rev 43:3–12.

Holmes TC, de Lacalle S, Su X, Liu G, Rich A, Zhang S (2000) Extensive neurite outgrowth and active synapse formation on self-assembling peptide scaffolds. Proc Natl Acad Sci USA 97:6728–6733.

Horii A, Wang X, Gelain F, Zhang S (2007) Biological designer self-assembling peptide nanofiber scaffolds significantly enhance osteoblast proliferation, differentiation and 3-D migration. PLoS One 2:e190.

Kiley P, Zhao X, Vaughn M, Baldo M, Bruce BD, Zhang S (2005) Self-assembling peptide detergents stabilize isolated photosystem I on a dry surface for an extended time. PLoS Biol 3:1181–1186.

Kisiday J, Jin M, Kurz B, Hung H, Semino C, Zhang S, Grodzinsky AJ (2002) Self-assembling peptide hydrogel fosters chondrocyte extracellular matrix production and cell division: implications for cartilage tissue repair. Proc Natl Acad Sci U S A 99:9996–10001.

Kleinman HK, McGarvey ML, Hassell JR, Star VL, Cannon FB, Laurie GW, et al. (1986) Basement membrane complexes with biological activity. Biochemistry 25:312–318.

Kleinman HK, Martin GR (2005) Matrigel: basement membrane matrix with biological activity. Semin Cancer Biol 15:378–386.

Kreis T, Vale R (1999) Guide book to the extracellular matrix, anchor, and adhesion proteins. 2nd ed. Oxford, UK: Oxford University Press.

Kubota Y, Kleinman HK, Martin GR, Lawley TJ (1988) Role of laminin and basement membrane in the morphological differentiation of human endothelial cells into capillary–like structures. J Cell Biol 107:1589–1598.

Lanza R, Langer R, VacantiJ (2000) Principles of Tissue Engineering 2nd edition. Academic Press: San Diego, CA.

Lee EY, Lee WH, Kaetzel CS, Parry G, Bissell MJ (1985) Interaction of mouse mammary epithelial cells with collagen substrata: regulation of casein gene expression and secretion. Proc Natl Acad Sci U S A 82:1419–1423.

Marini DM, Hwang W, Lauffenburger DA, Zhang S, Kamm RD (2002) Left-Handed Helical Ribbon Intermediates in the Self-Assembly of a β-Sheet Peptide. Nano Letters 2:295–299.

Nagai A, Nagai Y, Qu H, Zhang S (2007) Self-assembling behaviors of lipid-like peptides $A^6D$ and $A^6K$. J. Nanoscience & Nanotechnology 7:2246–2252.

Narmoneva DA, Oni O, Sieminski AL, Zhang S, Gertler JP, Kamm RD, Lee RT (2005) Self-assembling short oligopeptides and the promotion of angiogenesis. Biomaterials 26:4837–4846.

Oliver C, Waters JF, Tolbert CL, Kleinman HK (1987) Culture of parotid acinar cells on a reconstituted basement membrane substratum. J Dent Res 66:594–595.

Palsson B, Hubell J, Plonsey R, Bronzino JD (2003) Tissue engineering: Principles and applications in engineering. CRC Press: Boca Raton, FL

Pauling L (1960) The Nature of the Chemical Bond Third Edition. Cornell University Press: Ithaca, NY

Ratner B, Hoffman A, Schoen F, Lemons J (1996) Biomaterials Science. Academic Press: New York

Rich A, Davies D (1956) A new two-stranded helical structure: polyadenylic acid and polyuridylic acid. J Amer Chem Soc 78:3548.
Santoso S, Hwang W, Hartman H, Zhang S (2002) Self-assembly of surfactant-like peptides with variable glycine tails to form nanotubes and nanovesicles. Nano Letters 2:687–691.
Schmeichel KL, Bissell MJ (2003) Modeling tissue-specific signaling and organ function in three dimensions. J Cell Sci 116:2377–2388.
Timpl R, Rohde H, Robey PG, Rennard SI, Foidart JM, Martin GR (1979) Laminin--a glycoprotein from basement membranes. J Biol Chem 254:9933–9937.
Vauthey S, Santoso S, Gong H, Watson N, Zhang S (2002) Molecular self-assembly of surfactant-like peptides to form nanotubes and nanovesicles. Proc Natl Acad Sci USA 99:5355–5360.
von Maltzahn G, Vauthey S, Santoso S, Zhang S (2003) Positively charged surfactant-like peptides self-assemble into nanostructures. Langmuir 19:4332–4337.
Weaver VM, Howlett AR, Langton-Webster B, Petersen OW, Bissell MJ (1995) The development of a functionally relevant cell culture model of progressive human breast cancer. Semin Cancer Biol 6:175–184.
Yannas IV (2001) Tissue and organ regeneration in adults.
Yang S, Zhang S (2006) Self-assembling behavior of designer lipid-like peptides. Supramolecular Chemistry 18:389–396.
Yaghmur A, Laggner P, Zhang S, Rappolt M (2007) Tuning curvature and stability of monoolein bilayers by designer lipid-like peptide surfactants. PLoS ONE 2:e479.
Yeh JI, Du S, Tordajada A, Paulo J, Zhang S (2005) Peptergent: peptide detergents that improve stability and functionality of a membrane protein glycerol-3-phosphate dehydrogenase. Biochemistry 44:16912–16919.
Yokoi H, Kinoshita T, Zhang S (2005) Dynamic reassembly of peptide RADA16 nanofiber scaffold. Proc Natl Acad Sci U S A 102:8414–8419.
Zhang S (2002) Emerging biological materials through molecular self-assembly Biotechnology Advances 20:321–339.
Zhang S, Altman M (1999) Peptide self-assembly in functional polymer science and engineering. Reactive & Functional Polymers 41:91–102.
Zhang S, Lockshin C, Herbert A, Winter E, Rich A (1992) Zuotin, a putative Z-DNA binding protein in Saccharomyces cerevisiae. EMBO J 11:3787–3796.
Zhang S, Holmes T, Lockshin C, Rich A (1993) Spontaneous assembly of a self-complementary oligopeptide to form a stable macroscopic membrane. Proc Natl Acad Sci U S A 90:3334–3338.
Zhang S, Lockshin C, Cook R, Rich A (1994) Unusually stable beta-sheet formation in an ionic self-complementary oligopeptide. Biopolymers 34:663–672.
Zhang S, Holmes TC, DiPersio CM, Hynes RO, Su X, Rich A (1995) Self-complementary oligopeptide matrices support mammalian cell attachment. Biomaterials 16:1385–1393.
Zhang S, Zhao X, Spirio L (2005) PuraMatrix: Self-assembling peptide nanofiber scaffolds. In Scaffolding in Tissue Engineering. (Ed. Ma & Elisseeff) CRC Press, Boca Raton, FL pp.217–238.
Zhao X, Zhang S (2006) Self-assembling nanopeptides become a new type of biomaterial. Adv Polym Sci 203:145–170.
Zhao X, Nagai Y, Revees P, Kiley P, Khorana HG, Zhang S (2006) Designer lipid-like peptides significantly stabilize G-protein coupled receptor bovine rhodopsin. Proc Natl Acad Sci USA 103:17707–17712.
Zhau HE, Goodwin TJ, Chang SM, Baker TL, Chung LW (1997) Establishment of a three-dimensional human prostate organoid coculture under microgravity-simulated conditions: evaluation of androgen-induced growth and PSA expression. In Vitro Cell Dev Biol Anim 33:375–380.